# Numerical Solution of Steady Navier-Stokes Problems Using Integral Representations

C. M. Wang* and J. C. Wu†
*Georgia Institute of Technology, Atlanta, Georgia*

**Steady-state incompressible Navier-Stokes and continuity equations are recast into integral representations for the velocity and the vorticity vector using the concept of fundamental solutions. Integrals are discretized using finite Fourier series approximations. An efficient iterative procedure is established for the numerical solution of internal flow problems in two dimensions. The iteration loop in this procedure is composed of a kinetic step and a kinematic step. Explicit computations are utilized in each step. Boundary vorticity values required for the kinetic step are determined from constraint equations obtained from the kinematic aspect of the problem expressed in the integral representation form. Several flow problems are studied numerically for various Reynolds numbers. Flow structures are determined from numerical results obtained. A Bachelor's flow model of constant vorticity is verified numerically for high Reynolds number closed streamline flows inside a circle.**

## Introduction

DURING the past few years, the second author of this paper and his co-workers presented several articles[1-4] describing a method of the numerical solution of time-dependent incompressible viscous flow problems involving appreciable flow separations. This method utilizes the concept of vorticity and partitions the flow problem into its kinetic and kinematic aspects. The kinetic aspect is expressed as a differential transport equation describing the rate of change of vorticity through convective and diffusive processes. Knowing the velocity and vorticity distributions at any given instant of time, this kinetic equation permits the computation of a new vorticity distribution at a subsequent instant of time. The kinematic aspect determines the velocity distribution at any instant of time from known vorticity distribution at that instant. With the prevailing finite-difference and finite-element methods, the kinematics of the problem is expressed as a continuity equation and a definition of vorticity, or a Poisson equation, together with appropriate boundary conditions. With the new method, however, the kinematics of the problem is recast into an integral representation for the velocity or the stream function. The new method is named the integro-differential method.

With prevailing methods, implicit numerical procedures are necessary for the kinematic part of the computation. As a consequence, the solution field must include the entire flowfield, inclusive of the viscous and inviscid regions. It has been demonstrated, however, that the integral representations possess the distinguishing feature of permitting the explicit, point by point, computation of the velocity or the stream function values. This feature leads to several highly important attributes of the integro-differential method: 1) the solution field can be confined to the viscous region of the flow,[1] 2) the confined solution field can be segmented and each segment treated independently of the others,[3] and 3) numerical boundary conditions that presented difficulties in previous methods can be treated in a precise manner.[4]

Considerable experience has been gathered during the past few years in the implementation of the integro-differential method for studying various types of time-dependent viscous flow problems. The method was found to be particularly well suited for flows past finite solid bodies at moderate or high Reynolds numbers. For such flows, the computer time needed by prevailing methods is often prohibitive. The unique ability of the integro-differential method to confine the solution field to the viscous region is especially valuable since for such flows the viscous region generally occupies only a very small part of the total flowfield.

The integro-differential method was developed specifically for time-dependent viscous flow equations. Steady-state solutions, when desired, were obtained as asymptotic solutions of the time-dependent problem in the limit of large time. It has been noted that most of the successful numerical studies of the steady flow problem utilize the time-dependent equations as a vehicle for obtaining the desired steady solution asymptotically. While the time-dependent approach bypasses some of the great difficulties attendant on steady-state equations, it introduces an additional independent variable—the time—into solution procedure, and new difficulties have arisen in its application.

This paper reports on recent developments of a method that treats the steady viscous flow equations directly and, at the same time, retains the unique ability of the integro-differential method to confine the solution field to the viscous region of the flow. With this method, not only the kinematic aspect but also the kinetic aspect of the problem is recast into the form of integral representations. This method represents a major departure from previous methods for treating steady viscous flow problems and is named the integral representation method. The purpose of this paper is twofold: 1) to describe the integral representation formulation together with the associated solution procedure developed, and 2) to demonstrate by analysis and numerical illustrations that the integral representation method offers substantial advantages to the steady flow problem as does the integro-differential method to the time-dependent problem.

In numerical methods using the vorticity vector as a field variable, values of vorticity at flow boundaries need to be known in order to proceed with the computation. This vorticity boundary condition is usually determined by one-sided difference formulas using the no-slip condition at the boundary. Formulas of different orders of accuracy for determining these "extraneous boundary values"[4] are used by

Presented as Paper 85-0034 at the AIAA 23rd Aerospace Sciences Meeting, Reno, NV, Jan. 14-17, 1985; received April 24, 1985; revision received Dec. 4, 1985. 

*Post-Doctoral Fellow, School of Aerospace Engineering. Member AIAA.

†Professor, School of Aerospace Engineering. Associate Fellow AIAA.

different researchers. From a study of the biharmonic equations, which is a special case of the Navier-Stokes equations at zero Reynolds number, it is known that the approximations of boundary vorticity values significantly affect the accuracy of the numerical solution as well as the rate of convergence of the overall procedure.[5] It has been found that difference formulas of first-order accuracy tend to yield stable solutions while the second-order formulas tend to give unstable results at high Reynolds numbers.[6] The use of first-order formulas, however, restricts the overall accuracy of the solution.[4] An alternative approach, the velocity-pressure formulation, requires a knowledge of boundary values of the pressure gradient that is equivalent to the values of the boundary vorticity. The integral representation method overcomes the above difficulty. Boundary vorticities are determined by constraint equations imposed on the vorticity field. These constraint equations are derived through a kinematic consideration and are indeed the proper ones in accordance with a theorem offered by Quartapelle.[7]

The existence of Stokes solutions of internal flows indicates that an appropriate structure exists for the application of the series expansion of the field variables. Whereas finite-element methods are based on expansions in local basis functions, a series-expansion method based on expansion in global function is utilized in the present work. The spectral method is thus similar to the present method. The spectral method is, however, usually based on governing equations expressed in differential forms, e.g., Ref. 8, and satisfaction of the boundary conditions needs an approximation process in most cases. The present series-expansion method treats flow equations in their integral representation forms. With the integral representations, boundary conditions appear explicitly. In consequence, no approximation process other than those resulting from the discretization procedure is needed to satisfy the boundary conditions. Desirable properties of the spectral method are retained in the present approach. Specifically, if the solution of a flow problem is infinitely differentiable, the convergence of the spectral approximation will have an exponential rather than an algebraic character.[9] On the other hand, if the solution has only a finite number of derivatives $N$, the spectral approximation is expected to converge algebraically, that is, like some finite power of $1/N$. In general, the trigonometric series, the Cheybshev polynomials, and the Legendre polynomials have been used most often in the literature for spectral approximations.

With the present method, flow boundaries are mapped conformally onto a unit circle with the computation field mapped onto the interior of the circle. To demonstrate the validity and practicality of the new approach, geometries are kept simple and only flows generated by different velocity boundary conditions within circular boundaries are considered in this study. Although the flow geometry is relatively simple, a wide range of problems can be formulated, and many of them are of practical interest since it is possible to create various kinds of internal circulating and recirculating flows.

## Mathematical Formulation

### Kinematics and Kinetics

The incompressible motion of a viscous fluid is governed by the law of mass conservation and Newton's laws of motion. The mathematical statements of these two laws are familiarly expressed in differential forms in terms of the velocity field $v$ and the pressure field $p$, and are known respectively as the continuity and the Navier-Stokes equations.

It is convenient to replace the pressure field by the vorticity field and to partition the problem into its kinematic and kinetic aspects. This partition brings into focus a classical theorem concerning the kinematic aspect of flow problems[10]: "The motion of a fluid which occupied a limited simply connected region is determined when the values of the vorticity and the dilatation are known at all points in the region and the values of the normal velocity are known on the region's boundary."

The above theorem is valid for compressible and incompressible flows. For incompressible flows, the dilatation field is zero everywhere. In consequence, the velocity field is kinematically related only to the vorticity field. Specifically, differential equations describing the kinematic aspect of incompressible flow problems are the continuity equation and the definition of vorticity:

$$\nabla \cdot v = 0 \tag{1}$$

$$\nabla x v = \omega \tag{2}$$

where $v$ and $\omega$ are respectively the velocity vector and the vorticity vector.

If the vorticity field is known in a simply connected region $R$, then, according to the theorem stated earlier, the velocity is determined in $R$, provided that the normal component of the velocity vector is specified on the boundary $B$ of $R$. Equations (1) and (2) form an elliptic system of differential equations. The kinematic aspect of the problem therefore is a boundary value problem. The discretization of Eqs. (1) and (2) either by a finite-difference or a finite-element procedure yields a set of implicit algebraic equations. Using the concept of fundamental solutions, however, Eqs. (1) and (2) can be re-expressed in the form of an integral representation for the velocity vector. The discretization of this integral representation yields a set of explicit algebraic equations for velocity values.

The Navier-Stokes equations for a steady incompressible flow are

$$(v \cdot \nabla) v = -(1/\rho) \nabla p + \nu \nabla^2 v \tag{3}$$

where $\nu$ is the kinematic viscosity of the fluid, $\rho$ the density of the fluid, and $p$ the static pressure. In terms of vorticity, Eq. (3) can be rewritten as

$$\nabla x \omega = (1/\nu) v x \omega - (1/\nu) \nabla h \tag{4}$$

where $h$ is the total head defined by

$$h = p/\rho + v^2/2 \tag{5}$$

where $v$ is the magnitude of the velocity vector $v$.

The vorticity is solenoidal since it is the curl of a vector field, i.e., the velocity field. One therefore has

$$\nabla \cdot \omega = 0 \tag{6}$$

Equations (4) and (6) describe the kinetic aspect of the incompressible flow problem. Equations (4) and (6) bear a formal resemblance to Eqs. (2) and (1). The kinetic aspect of the problem is therefore a boundary value problem. This kinetic aspect is also expressible as a vorticity transport equation by taking the curl of Eq. (4) and using Eq. (6). With a finite-difference or a finite-element procedure, an iterative procedure is usually used to advance the solution from an old iteration level to a new iteration level through a computational loop consisting of the following two parts:

1) With known velocity and vorticity values at the old iteration level, the vorticity transport equation is solved to obtain interior vorticity values at the new iteration level.

2) With new vorticity values already computed, Eqs. (1) and (2) are solved to obtain velocity values at the new iteration level.

Part 1 is the kinetic part of the computational loop. Since the kinetic aspect of the problem is a boundary value problem, proper boundary conditions for the vorticity vector must be specified before part 1 can be carried out. This boundary condition is not given by the kinetic aspect of the problem.[4] Rather, it is a consequence of the kinematic aspect of the problem, as will be discussed later in this section in connection with the integral representations.

**Integral Representations**

Using the concept of fundamental solution of elliptic equations, Eqs. (1) and (2) can be recast into an integral representation for the velocity vector[2]

$$v(r) = -\frac{1}{2\pi}\int_R \frac{\omega_0 x(r_0 - r)}{|r_0 - r|^2}dR_0 + \frac{1}{2\pi}\oint_B \frac{(v_0 \cdot n_0)(r_0 - r)}{|r_0 - r|^2}dB_0 - \frac{1}{2\pi}\oint_B \frac{(v_0 x n_0)x(r_0 - r)}{|r_0 - r|^2}dB_0 \tag{7}$$

where $r$ is a position vector and $n$ the unit normal vector on the boundary $B$ directed outward. The subscript 0 indicates that a variable or an integration is taken in the $r_0$ space; for example, $\omega_0 = \omega(r_0)$. The first integral in Eq. (7) is an expression of the Biot-Savart law for distributed vorticity in the region $R$. The two boundary integrals represent contributions from velocity boundary conditions.

Noting the formal resemblance between the set of Eqs. (4) and (6) and the set of Eqs. (2) and (1), one obtains, by replacing $v$ in Eq. (7) by $\omega$ and replacing $\omega$ in Eq. (7) by $1/\nu(vx\omega - \nabla h)$, an integral representation for the vorticity vector

$$\omega(r) = -\frac{1}{2\pi\nu}\int_R \frac{(v_0 x\omega_0)x(r_0 - r)}{|r_0 - r|^2}dR_0 + \frac{1}{2\pi\nu}\int_R \frac{\nabla_0 h_0 x(r_0 - r)}{|r_0 - r|^2}dR_0 - \frac{1}{2\pi}\oint_B \frac{(\omega_0 x n_0)x(r_0 - r)}{|r_0 - r|^2}dB_0 \tag{8}$$

The integrand of the second integral in Eq. (8) can be rewritten as

$$\nabla_0 x\left[\frac{h_0(r_0 - r)}{|r_0 - r|^2}\right]$$

By the use of the Gauss theorem, the second integral in Eq. (8) can be reexpressed as a boundary integral. Equation (8) then becomes

$$\omega(r) = -\frac{1}{2\pi\nu}\int_R \frac{(v_0 x\omega_0)x(r_0 - r)}{|r_0 - r|^2}dR_0 + \frac{1}{2\pi\nu}\oint_B \frac{h_0 n_0 x(r_0 - r)}{|r_0 - r|^2}dB_0 - \frac{1}{2\pi}\oint_B \frac{(\omega_0 x n_0)x(r_0 - r)}{|r_0 - r|^2}dB_0 \tag{9}$$

The first integral in Eq. (9) represents the contribution of the convective process to the vorticity field. The second integral represents the contribution of the total head on flow boundary. The last integral in Eq. (9) is a boundary integral giving the contribution of the vorticity boundary condition. During each iteration in a computation procedure, known velocity and vorticity values at the old iteration level can be utilized to evaluate the integrals on the right-hand sides of Eqs. (7) and (9). Values of vorticity and velocity at the new iteration level are then expressed explicitly as a function of known values and can be evaluated point by point.

Equations (7) and (9) can be modified for three-dimensional flows by replacing the denominator of each integrand by $|r_0 - r|^3$, dividing each term by the factor of 2 and adding[1]

$$\frac{1}{4\pi}\oint_B \frac{(\omega_0 \cdot n_0)(r_0 - r)}{|r_0 - r|^3}dB_0$$

**Boundary Conditions**

According to the theorem stated earlier, if a vorticity field is known in a simply connected region $R$, then the following velocity condition on the boundary $B$ is sufficient for the determination of the velocity field in $R$ uniquely:

$$v \cdot n = f(r_B) \tag{10}$$

where $r_B$ is a position vector on $B$ and $f$ is a known function of $r_B$. If the region is multiply connected, then the value of circulation in the several independent circuits of the region must also be specified. It has been shown[11] that the following boundary condition is also sufficient for the unique determination of $v$ in $R$:

$$vxn = g(r_B) \tag{11}$$

where $g$ is a known function of $r_B$. Although either Eq. (10) or (11) is sufficient, the use of both conditions (10) and (11) in a numerical procedure is permitted if the two conditions are compatible with each other; otherwise the kinematic aspect of the flow problem is overspecified.[4]

In general, both conditions (10) and (11) are established from the physics of the problem, and therefore the compatibility of the two conditions are assured. However, this compatibility does not exist for all vorticity fields in $R$. In other words, since both conditions (10) and (11) are contained in Eq. (7), the vorticity field in $R$ is subject to a kinematic restriction.

Quartapelle[7] suggested a theorem on the kinematic restriction. He expressed this restriction in the form of a constraint equation:

$$\int_R \omega\tau dR = \oint_B \left(\frac{\partial\psi}{\partial n}\tau - \psi\frac{\partial\tau}{\partial n}\right)dB \tag{12}$$

where $\tau$ is an arbitrary harmonic function and $\psi$ is a stream function. It can be shown that this constraint equation is obtainable from Eq. (7). In the present work, Eq. (7) is applied to the boundary points $r_B$, yielding

$$v(r_B) = -\frac{1}{2\pi}\int_R \frac{\omega_0 x(r_0 - r_B)}{|r_0 - r_B|^2}dR_0 + \frac{1}{2\pi}\oint_B \frac{(v_0 \cdot n_0)(r_0 - r_B)}{|r_0 - r_B|^2}dB_0 - \frac{1}{2\pi}\oint_B \frac{(v_0 x n_0)x(r_0 - r_B)}{|r_0 - r_B|^2}dB_0 \tag{13}$$

With $v \cdot n$ and $vxn$ both known on $B$, the left-hand side as well as the two boundary integrals in Eq. (13) are known. Therefore, Eq. (13) represents a constraint on the value of the first integral. That is, the vorticity distribution in $R$ is restricted kinematically by Eq. (13). In the present work, this kinematic restriction is used to determine the vorticity boundary condition.[4] Specifically, in the kinematic part of a computation loop, i.e., part 2 described earlier, the interior values of $\omega$ are known from the kinetic part (part 1 of the computation loop). In Eq. (13) the boundary values of $v$ are given. The only unknown values are the boundary values of $\omega$. Equation (13) therefore gives an integral equation to determine the vorticity boundary values. After the boundary values of $\omega$ are determined, they are used in Eq. (7) to compute the interior values of $v$. The kinematic part of the computation loop therefore is composed of two steps. In the first step, known interior values of vorticity and known boundary values of velocity are used to compute boundary values of vorticity. In the second step, known interior and boundary values of vorticity and known boundary values of velocity are used to compute interior values of velocity.

The kinetic part of the computation loop is similarly divided into two steps. In the first step, Eq. (9) is applied to the boundary points $r_B$. With boundary and interior values of vorticity as well as the interior values of velocity determined from the preceding iteration, this specialized equation contains only boundary values of the total head as the unknowns. After the boundary values of the total head are computed, the new interior values of vorticity are calculated using Eq. (9).

**Series Expansions**

In the present study, integral representations are utilized in the computation of two-dimensional flows inside a unit circle. A polar coordinate system $(r, \theta)$ is used in the planes of the flow. Field variables are approximated by finite Fourier series along the azimuthal direction as follows:

$$v_r = a_0(r) + \sum_{n=1}^{N} [a_n(r)\cos n\theta + b_n(r)\sin n\theta] \tag{14}$$

$$v_\theta = c_0(r) + \sum_{n=1}^{N} [c_n(r)\cos n\theta + d_n(r)\sin n\theta] \tag{15}$$

$$\omega = \alpha_0(r) + \sum_{n=1}^{N} [\alpha_n(r)\cos n\theta + \beta_n(r)\sin n\theta] \tag{16}$$

After substituting these equations into the integral representations for the velocity and the vorticity, the following integral relations are then obtained from the Fourier coefficients[12]:

$$a_0 = 0 \tag{17}$$

$$a_n = \frac{1}{2}\int_0^r \beta_n \left(\frac{r_0}{r}\right)^{n+1} dr_0 + \frac{1}{2}\int_r^1 \beta_n \left(\frac{r}{r_0}\right)^{n-1} dr_0 + \frac{1}{2}a_n(1)r^{n-1} - \frac{1}{2}d_n(1)r^{n-1} \tag{18}$$

$$b_n = -\frac{1}{2}\int_0^r \alpha_n \left(\frac{r_0}{r}\right)^{n+1} dr_0 - \frac{1}{2}\int_r^1 \alpha_n \left(\frac{r}{r_0}\right)^{n-1} dr_0 + \frac{1}{2}b_n(1)r^{n-1} + \frac{1}{2}c_n(1)r^{n-1} \tag{19}$$

$$c_0 = \int_0^r \alpha_0 \left(\frac{r_0}{r}\right) dr_0 \tag{20}$$

$$c_n = \frac{1}{2}\int_0^r \alpha_n \left(\frac{r_0}{r}\right)^{n+1} dr_0 - \frac{1}{2}\int_r^1 \alpha_n \left(\frac{r}{r_0}\right)^{n-1} dr_0 + \frac{1}{2}b_n(1)r^{n-1} + \frac{1}{2}c_n(1)r^{n-1} \tag{21}$$

$$d_n = \frac{1}{2}\int_0^r \beta_n \left(\frac{r_0}{r}\right)^{n+1} dr_0 - \frac{1}{2}\int_r^1 \beta_n \left(\frac{r}{r_0}\right)^{n-1} dr_0 - \frac{1}{2}a_n(1)r^{n-1} + \frac{1}{2}d_n(1)r^{n-1} \tag{22}$$

$$\alpha_0 = \alpha_0(1) - \frac{1}{\nu}\int_r^1 \xi_0 dr_0 \tag{23}$$

$$\alpha_n = \alpha_n(1)r^n - \frac{1}{2\nu}\int_0^1 (\xi_n - \zeta_n) r^n r_0^n dr_0 + \frac{1}{2\nu}\int_0^r (\xi_n - \zeta_n)\left(\frac{r_0}{r}\right)^n dr_0 - \frac{1}{2\nu}\int_r^1 (\xi_n + \zeta_n)\left(\frac{r}{r_0}\right)^n dr_0 \tag{24}$$

$$\beta_n = \beta_n(1)r^n - \frac{1}{2\nu}\int_0^1 (\eta_n + \mu_n) r^n r_0^n dr_0 + \frac{1}{2\nu}\int_0^r (\eta_n + \mu_n)\left(\frac{r_0}{r}\right)^n dr_0 + \frac{1}{2\nu}\int_r^1 (\mu_n - \eta_n)\left(\frac{r}{r_0}\right)^n dr_0 \tag{25}$$

where $a_n(1)$, $b_n(1)$, $c_n(1)$, and $d_n(1)$ are the velocity Fourier coefficients on the flow boundary ($r=1$), and $\xi$, $\eta$, $\zeta$, and $\mu$ are the Fourier coefficients of the convective terms defined by

$$\omega v_r = \xi_0(r) + \sum_{n=1}^{N} [\xi_n(r)\cos n\theta + \eta_n(r)\sin n\theta] \tag{26}$$

$$\omega v_\theta = \mu_0(r) + \sum_{n=1}^{N} [\mu_n(r)\cos n\theta + \zeta_n(r)\sin n\theta] \tag{27}$$

For convenience in computational procedures, as described later in this paper, the convective terms are expressed in the form of Eqs. (26) and (27), instead of the product of Eqs. (16) with Eqs. (14) and (15).

It is worthy of note that Eq. (17) is a consequence of the continuity equation, which permits no net flow across any closed path in the flow domain. That is, Eq. (1) gives

$$\oint_c v_n ds = 0 \tag{28}$$

where $c$ is a closed path in $R$. Therefore, using Eq. (14) and letting $c$ be a circle, one obtains

$$\oint_c r a_0(r) d\theta = 0 \tag{29}$$

which requires $a_0(r) = 0$.

It is also worthy of note that the Navier-Stokes equations, expressed in the form of Eq. (4), yield the following integral relation

$$\oint \omega \boldsymbol{v}\cdot\boldsymbol{n} ds = \nu \oint \nabla\omega\cdot\boldsymbol{n} ds \tag{30}$$

Using Eqs. (16) and (26), it is easy to show that Eq. (30) yields Eq. (23). Equation (30) is sometimes regarded as an expression of the conservation of vorticity in viscous flow.

Fourier coefficients of the boundary vorticity, $\alpha_0(1)$, $\alpha_n(1)$, and $\beta_n(1)$, are needed to evaluate the interior vorticity values. These coefficients are determined by the following constraint equations:

$$\int_0^1 \alpha_0 r_0 dr_0 = c_0(1) \tag{31}$$

$$\int_0^1 \alpha_n r_0^{n+1} dr_0 = c_n(1) - b_n(1), \qquad 1 \le n \le N \tag{32}$$

$$\int_0^1 \beta_n r_0^{n+1} dr_0 = a_n(1) + d_n(1), \qquad 1 \le n \le N \tag{33}$$

The above relations satisfy the kinematic restriction on the vorticity distribution as discussed earlier. That is, these relations provide a linkage between the kinematics and the kinetics in the iterative numerical solution procedure of a flow problem.

## Solution Procedure

The set of Eqs. (18-25) relates the Fourier coefficients of field variables $v_r$, $v_\theta$, $\omega$, $\omega v_r$, and $\omega v_\theta$. These equations are subject to constraints given by Eqs. (31-33). The solution of this set of equations yields values of the Fourier coefficients $a_n(r)$, $b_n(r)$, etc., which, when placed into Eqs. (14-16), (26), and (27) gives the values of the field variables $v_n$, $v_\theta$, $\omega$, etc. The numerical solution of this set of equations is quite simple since only one-dimensional quadratures, in the radial direction, are involved. In the present work, the integrals in this set of equations are discretized using either an evenly spaced grid or a Chebyshev grid in the radial direction. The Chebyshev grid is well suited for computation of high Reynolds number flows because it provides closer spacing between grid points near the flow boundary, i.e.,

$$r_j = 1 - \cos(j\pi/2M), \quad j = 0,\ 1, \ldots, M \tag{34}$$

where $M$ is the number of grid spacings in the radial direction.

Since the kinetic aspect of the problem is nonlinear, an iterative approach is required. In the present work, a suitably assumed vorticity distribution in the interior of the fluid domain is utilized to initiate the solution. Fourier coefficients for the assumed interior vorticity are determined using Eq. (16). Fourier coefficients $a_n(1)$, $b_n(1)$, $c_n(1)$, and $d_n(1)$ for the boundary velocities are determined using Eqs. (14) and (15) and prescribed velocity boundary conditions. The kinetic and the kinematic aspects are then alternatively solved and the kinematic restriction described in the preceding section is utilized to establish the needed vorticity boundary condition. The following computational steps constitute a complete iterative loop that advances the solution field from an old iteration level to a new one:

1) With known Fourier coefficients for the interior vorticity and the boundary velocity, Fourier coefficients for the boundary vorticity are determined by the kinematic constraints, Eqs. (31-33).

2) Fourier coefficients for the velocity field are then computed using the kinematic integral relations, Eqs. (17-22).

3) Fourier coefficients for the convective terms are computed using Eqs. (26) and (27). Note that $\mu_0$ need not be determined.

4) Compute Fourier coefficients for the interior vorticity for the next iteration level using Eqs. (23-25).

A point underrelaxation technique is employed to obtain converged solutions. New values of Fourier coefficients for the interior vorticity are computed by using

$$\alpha_0^{i+1} = \lambda_0 \alpha_0^* + (1-\lambda_0)\alpha_0^i \tag{35}$$

$$\alpha_n^{i+1} = \lambda\alpha_n^* + (1-\lambda)\alpha_n^i, \quad 1 \le n \le N \tag{36}$$

$$\beta_n^{i+1} = \lambda\beta_n^* + (1-\lambda)\beta_n^i, \quad 1 \le n \le N \tag{37}$$

where $\lambda_0$, $\lambda$ are underrelaxation parameters and the superscript $i$ denotes the $i$th iteration level. $\alpha_0^*$, $\alpha_n^*$, and $\beta_n^*$ are intermediate values computed from step 4. The iterative procedure stops if the following criterion of maximum deviation of the vorticity Fourier coefficients is satisfied

$$D_{\max} = \max_j |\alpha_{0,j}^{i+1} - \alpha_{0,j}^i, \alpha_{n,j}^{i+1} - \alpha_{n,j}^i, \beta_{n,j}^{i+1} - \beta_{n,j}^i| \le \epsilon \tag{38}$$

where the subscript $j$ denotes the values of Fourier coefficients at $r = r_j$. The prescribed value of $\epsilon$ is set to be $10^{-4}$ in the present study.

## Results and Discussions

Current literature contains a large number of articles dealing with numerical studies of flows external to circular boundaries. Internal flows within circular boundaries, however, have received relatively little attention. Kuwahara and Imai[13] computed several flow problems at low and moderate Reynolds numbers. The highest Reynolds number that has been successfully computed in Ref. 13 is 1024. For high Reynolds number flows, previous investigators either treated linearized Navier-Stokes equations[14] or employed a hypothesis of constant vorticity core.[15,16] In this paper, solutions of high Reynolds number flows are accomplished by decomposing the overall flow into a basic flow and a disturbance flow utilizing the concept of a constant core vorticity. With the circular geometry, the appropriate basic flow to use is that of a solidlike rotational flow. The decomposition procedure makes the solution of high Reynolds number flow a relatively simple task with fast convergence. It should phasized that the decomposition procedure employed is easily achieved through the use of integral representation[12] and does not imply a linearization or a small perturbation concept. Rather, the full Navier-Stokes equations are solved.

The numerical solutions at low and moderate Reynolds numbers are carried out using uniform grids along the radial direction. The radial axis is divided into $M$ intervals. Different values of $M$ are used to study the rate of convergence of the procedure. Chebyshev grids are used for high Reynolds number computations. The use of Chebyshev grids adds only a small amount of excess computational work through the numerical quadrature on integral relations, compared with the use of uniform grids. Numerical solutions for selected flow problems are presented below.

### Flow Without Separation

Boundary velocities for this problem are given by

$$(v_r)_B = 0 \tag{39}$$

$$(v_\theta)_B = 1/2 + 1/2\cos\theta \tag{40}$$

Based on extensive numerical studies, a uniform grid with $M = 20$ is sufficient for low and moderate Reynolds numbers. The number of trigonometric functions used, $N$, is selected to be 20 for sufficient resolution in the azimuthal direction. The smaller values of underrelaxation parameters should be used at higher Reynolds numbers and on finer grids. Several flow characteristics at $R_e = 1000$ computed using different grids are presented in Table 1.

Solutions obtained using a Chebyshev grid with $M = 20$ are approximately equivalent to solutions obtained using a uniform grid with $M = 58$. Differences in flow variables computed using Chebyshev grids $M = 20$ and $M = 40$ are within 1%. It is obvious from Table 2 that the uniform grid is undesirable for higher Reynolds numbers.

From present calculations, it is found that an increase of grid points by a factor of two using the Chebyshev grid permits the flow Reynolds number of the flow to increase by a factor of 10. Chebyshev grids with $M = 20$, 40, and 60 are respectively adequate for flows at $R_e = 10^3$, $10^4$, and $10^5$.

Results obtained in the present study are in excellent agreement with those obtained in Ref. 13 up to a Reynolds

**Table 1 Flow characteristics at $R_e = 1000$**

| | Uniform grids | | | Chebyshev grids | | |
|---|---|---|---|---|---|---|
| $M$ | 20 | 40 | 60 | 20 | 30 | 40 |
| $\omega(r=0)$ | 1.194 | 1.249 | 1.259 | 1.255 | 1.262 | 1.264 |
| $\omega_{\max}$ | 12.282 | 13.548 | 13.762 | 13.757 | 13.821 | 13.843 |
| $\psi(r=0)$ | .289 | .300 | .303 | .301 | .303 | .303 |
| $\alpha_0(0)$ | 1.194 | 1.248 | 1.259 | 1.255 | 1.262 | 1.264 |

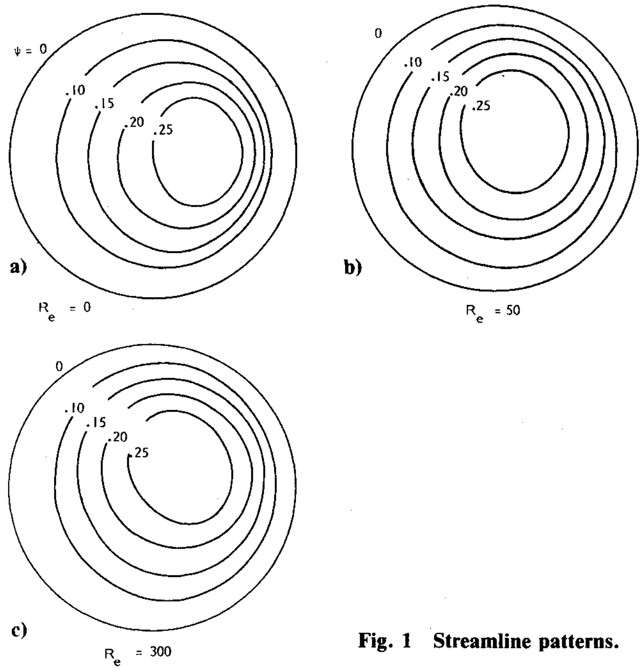


Fig. 1 Streamline patterns.

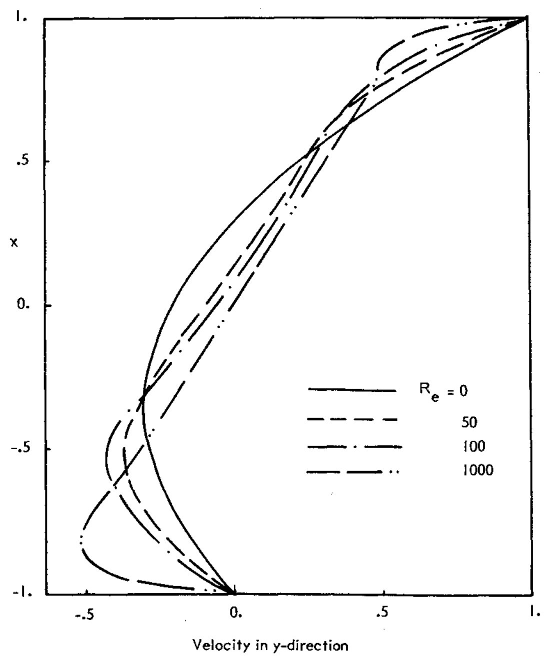


Fig. 2 Velocity distribution on $x$ axis.

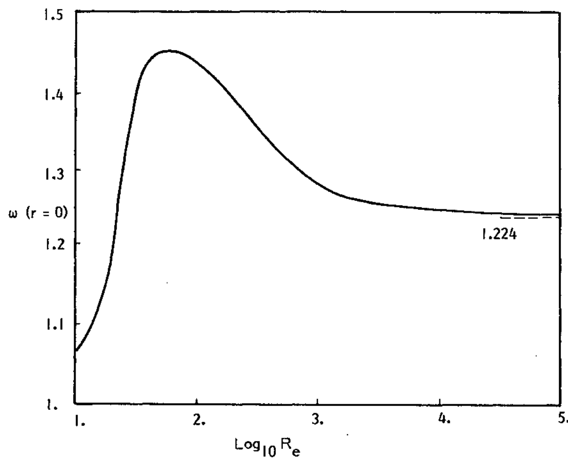


Fig. 3 Convergence of vorticity value in inviscid region.

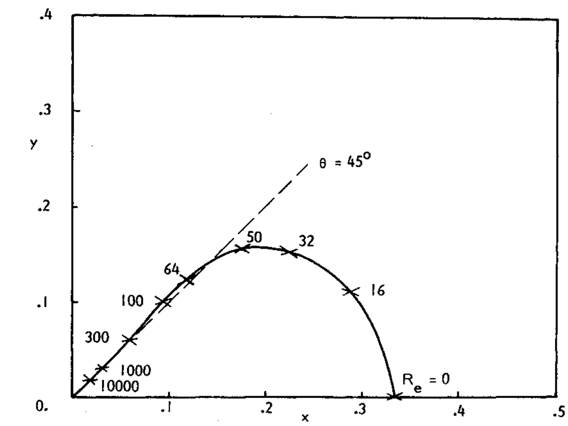


Fig. 4 Migration of vortex center.

Table 2 Flow characteristics at $R_e = 10^4$

| | Uniform grids | | | Chebyshev grids | | |
|---|---|---|---|---|---|---|
| $M$ | 50 | 70 | 90 | 40 | 50 | 60 |
| $\omega(r=0)$ | 1.143 | 1.185 | 1.205 | 1.229 | 1.232 | 1.234 |
| $\omega_{max}$ | 33.322 | 36.601 | 38.266 | 40.077 | 40.194 | 40.257 |
| $\psi(r=0)$ | .283 | .293 | .298 | .304 | .304 | .305 |
| $\alpha_0(0)$ | 1.143 | 1.185 | 1.205 | 1.229 | 1.232 | 1.234 |

number of 1000. For high Reynolds number calculations, the basic flow is selected as a solidlike rotation with unit angular velocity. The computer time consumed for high Reynolds number calculations is virtually independent of the flow Reynolds number. Approximately 25 s of CDC 855 CPU time are used for each high Reynolds number calculation.

Streamlines for different Reynolds numbers are shown in Fig. 1. As the Reynolds number increases, the flow pattern becomes unsymmetric, and the vortex center is shifted in the direction of the moving boundary, due to the nonlinear inertial effect. A straight part of the velocity profile (Fig. 2) indicates the region of nearly constant vorticity. Viscous stresses are negligible in this region. The vorticity value of this core region converges to an asymptotic value as the Reynolds number increases, as shown in Fig. 3. This asymptotic value is the same as the value calculated analytically from the flow model suggested by Bachelor,[15] which is $(3/2)^{1/2}$. The migration of the vortex center is shown in Fig. 4. At high Reynolds numbers, the inertial effect becomes dominant, and the vortex center tends to align with the center of the circle.

#### Flow with a Step Boundary Tangential Velocity

Boundary velocities for this problem are given by

$$(v_r)_B = 0 \tag{41}$$

$$\begin{aligned}(v_\theta)_B &= 1, \qquad -\pi/4 < \theta < \pi/4 \\ &= 0, \qquad \pi/4 < \theta < 2\pi - \pi/4\end{aligned} \tag{42}$$

Chebyshev grids with $M = 20$ and 40 are going to be sufficient for the case of $R_e = 10^3$ and $10^4$, respectively. Because the tangential boundary velocity is piecewise continuous, a larger value of $N$ is required to represent the flow near the boundary adequately. As observed in the previous problem, a constant vorticity core is established in the center region. The flow region is therefore segmented into an inner and an

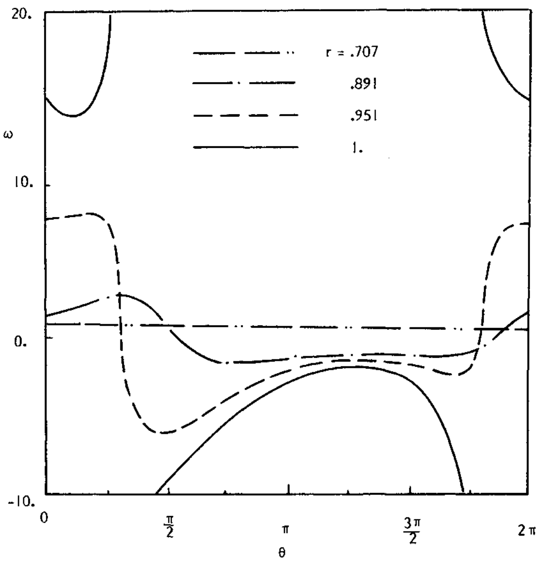


**Fig. 5 Vorticity distribution along circumferential direction ($R_e = 1000$).**

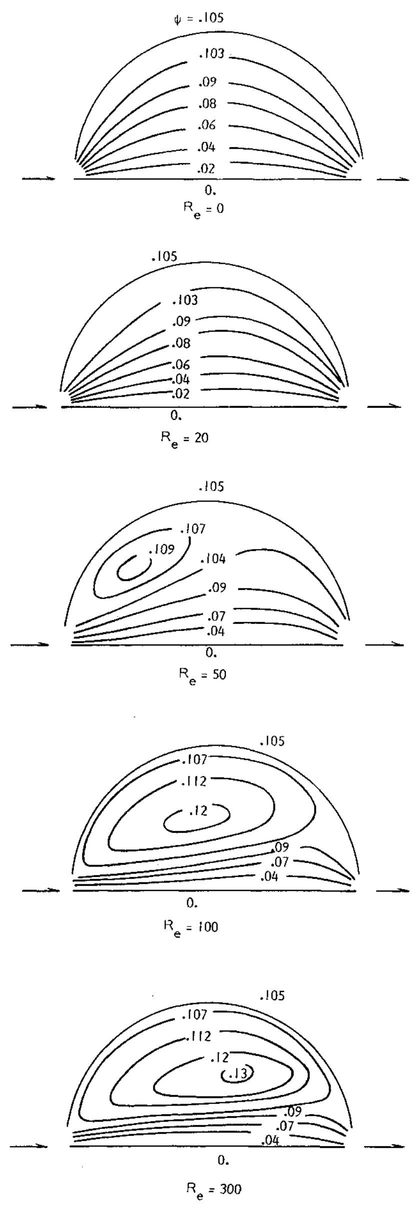


**Fig. 6 Streamline patterns.**

outer part in the present computation. In the inner region, $N$ is set to be 10. In the outer region, $N$ is set to be 60. This segmentation not only has the advantage of saving computer time but also requires a smaller data storage requirement. The radial position that segments the flow region is selected in accordance with the flow Reynolds number.

The vorticity distribution along the azimuthal direction (Fig. 5) shows the singular behavior at the flow boundary, which is the consequence of the discontinuities of the tangential boundary velocity at $\theta = \pi/4$ and $-\pi/4$. The large variation along the $\theta$ direction decays across the boundary layer due to viscous effects, and the vorticity rapidly approaches a constant value. This constant value is unity if determined from Bachelor's model, which is numerically proved to be true by present computations.

### Flow with Prescribed Inlet-Outlet Velocities

Boundary velocities for this problem are given by

$$(v_r)_B = 1, \quad -\alpha/2 < \theta < \alpha/2$$

$$= -1, \quad \pi - \alpha/2 < \theta < \pi + \alpha/2; \; \alpha = 6 \text{ deg}$$

$$= 0, \quad \text{otherwise} \tag{43}$$

$$(v_\theta)_B = 0 \tag{44}$$

Since the flow is symmetric about $\theta = 0$ and $\pi$, only the upper half of the flow domain needs to be computed and the Fourier series expansions of the field variables can be simplified, e.g.,

$$\omega = \sum_{n=1}^{N} \beta_n \sin n\theta \tag{45}$$

The computations are performed on a uniform grid with $M = 20$ for different Reynolds numbers from 0 to 300. The streamline patterns (Fig. 6) show that the flow is symmetric about $\theta = \pi/2$ for $R_e = 0$ and becomes unsymmetric at higher Reynolds numbers. As the Reynolds number increases, recirculation occurs and the separation bubble shifts downstream as the inertial effect increases with the Reynolds number.

## Conclusions

Numerical results obtained and computer times used in the present study indicate that the present method offers remarkable solution speed and accuracy. Furthermore, the computer storage requirements for the present method are small. The advantages of high accuracy associated with spectral methods are available to the present method. For high Reynolds number cases, solutions obtained using Chebyshev grids converge rapidly and solutions computed using uniform grids converge relatively slowly.

At a high flow Reynolds number, the flow takes on a boundary-layer characteristic. Vorticity gradients are appreciable only in a narrow region near the flow boundary at high Reynolds numbers. Based on the numerical results obtained, it is concluded that Bachelor's flow model of constant vorticity is valid for closed streamline flows.

Flows inside square domains have been computed by using Chebyshev polynomials to discretize the integral representations.[12] Using the methods of conformal mapping and flowfield segmentation, flows within complex geometries can be treated while preserving the advantageous properties of the present method.

## Acknowledgments

This paper is prepared under support by ARO, Contract No. DAAG-29-82-K-0094.

## References

[1]Wu, J. C. and Thompson, J. F., "Numerical Solution of Time Dependent Incompressible Navier-Stokes Equations Using an Integro-Differential Formulation," *Computers and Fluids*, Vol. 1, No. 2, 1973, pp. 197-215.

[2]Wu, J. C., "Integral Representations of Fluid Variables for the Finite Element Solution of Viscous Flow Problems," *Proceedings of the 1974 Conference on Finite Element Methods in Engineering*, Oxford University Press, (Clarendon Press), Oxford, England, 1974, pp. 827-840.

[3]Wu, J. C., Sampath, S., and Sankar, N. L., "A Numerical Study of Viscous Flows Around Airfoils," *The AGARD Fluid Dynamics Panels Symposium on Unsteady Aerodynamics*, AGARD-CP-227, Ottawa, Canada, Sept. 1977.

[4]Wu, J. C., "Numerical Boundary Conditions for Viscous Flow Problems," *AIAA Journal*, Vol. 14, Aug. 1976, pp. 1042-1049.

[5]Gupta, M. M., "Discretization Error Estimates for Certain Splitting Procedures for Solving First Biharmonic Boundary Value Problems," *SIAM Journal of Numerical Analysis*, Vol. 12, No. 3, 1975, pp. 364-371.

[6]Gupta, M. M. and Manohar, R. P., "Boundary Approximations and Accuracy in Viscous Flow Computations," *Journal of Computational Physics*, Vol. 31, May 1979, pp. 265-288.

[7]Quartapelle, L., "Vorticity Conditioning in the Computation of Two-Dimensional Viscous Flows," *Journal of Computational Physics*, Vol. 40, April 1981, p. 453-477.

[8]Gottlieb, D. and Orszag, S. A., *Numerical Analysis of Specral Methods: Theory and Applications*, Regional Conference in Applied Mathematics, published by Society for Industrial and Applied Mathematics, Philadelphia, 1977.

[9]Haidvogal, D. B. and Zang, T., "The Accurate Solution of Poisson's Equation by Expansion in Chebyshev Polynomials," *Journal of Computational Physics*, Vol. 30, Feb. 1979, pp. 167-180.

[10]Lamb, H., *Hydrodynamics*, Dover Publications, New York, 1945.

[11]Wu, J. C. and Gulcat, U., "Separate Treatment of Attached and Detached Flow Regions in General Viscous Flows," *AIAA Journal*, Vol. 19, Jan. 1981, pp. 20-27.

[12]Wang, C. M., "Computation of Steady Internal Flows Using Integral Representation Method with Finite Series Expansions," Ph.D. Thesis, Georgia Institute of Technology, Atlanta, GA, 1983.

[13]Kuwahara, K. and Imai, I., "Steady Viscous Flows Within a Circular Boundary," *The Physics of Fluids*, Supplement II, 1969, pp. 94-101.

[14]Burggraf, O. R., "Analytical and Numerical Studies of the Structure of Steady Separated Flows," *Journal of Fluid Mechanics*, Vol. 24, Jan. 1966, pp. 113-151.

[15]Bachelor, G. K., "On Steady Laminar Flow with Closed Streamlines at Large Reynolds Numbers," *Journal of Fluid Mechanics*, Vol. 2, Jan. 1957, pp. 77-87.

[16]Squire, H. B., "Note on the Motion Inside a Region of Recirculation," *Journal of the Royal Aeronautical Society*, Vol. 60, March 1956, pp. 203-205.